Two-State Description of Stochastic Excitability

Benjamin Lindner*, Lars Meinhold† and Lutz Schimansky-Geier**

*Department of Physics, University of Ottawa, 150 Louis Pasteur, Ottawa, Canada KIN 6N5
†IWR - Biocomputing, Heidelberg University, Im Neuenheimer Feld 368, D-69120 Heidelberg
**Institute of Physics, Humboldt-University of Berlin, Invalidenstr. 110, D-10115 Berlin

Abstract. We review analytic results of two-state dynamics that results from the approximation of excitable dynamics. By means of power spectrum, coeffient of variation and diffusion coefficient of the number of excitations we demonstrate coherence resonance in the Fitzhugh-Nagumo model and in a cluster of calcium ion channels.

INTRODUCTION

Excitability is encountered in fi elds as different as neurobiology and physical chemistry. It is commonly described by two-dimensional dynamical systems that respond to stimulation in an all-or-none fashion, i.e. either the input strength suffi ces to elucidate a strong nonlinear response (spike or pulse seen in one of the variables) or the system remains essentially silent. When noise is present in such an excitable system, unexpected phenomena like coherence resonance (CR) can be observed: the excitation sequence (pulse train) is most regular for a fi nite (optimal) amount of input noise [1]. This can be easily verifi ed in computer simulations of the activator-inhibitor system; the effect is, however, more complicated to treat analytically at this level.
Here we show analytic results for CR in two different two-dimensional models using a two-state description of stochastic excitability. First, we will study the stochastic FitzHugh-Nagumo (FN) neuron model and explain the main idea of our approximation. Second, we consider a model for a cluster of calcium ion channels. The origin of noise is quite different in these two systems: while in the FN model noise is mainly given by random synaptic input, fluctuations occurring in the calcium dynamics are due to the fi nite number of interacting channels and hence in this case we deal with internal noise.

STOCHASTIC FITZHUGH-NAGUMO MODEL

This model is frequently used in computational studies of neurons. In terms of the fast voltage (or activator) variable $v(t)$ and the slow recovery (or inhibitor) variable $u(t)$ it reads

$$\tau\dot{v} = F(v) - u, \quad \dot{u} = \gamma v - u + b + \sqrt{2D}\xi(t) \tag{1}$$

where $\xi(t)$ is Gaussian white noise, τ is the (small) time scale ratio of the two variables and b is a constant determining positions of the null clines $u = F(v)$ and $u = \gamma v + b$.

The nonlinearity in v is either given by a cubic function $F(v) = v - v^3$ or by a piecewise linear approximation of it

$$F_{pwl}(v) = \begin{cases} -1 - v & , \quad v \leq -1/2 \\ v & , \quad -1/2 < v < 1/2 \\ +1 - v & , \quad v \geq 1/2 \end{cases} \tag{2}$$

Under the influence of the noise the model generates spikes in the voltage variable that are separated by the so called interspike intervals (cf. Fig. 1, l.h.s.). How can the regularity of this spike sequence be quantified?
First, we may consider the statistics of the interspike interval, in particular its relative standard deviation, also known as coefficient of variation (CV)

$$R = \sqrt{\langle T^2 \rangle - \langle T \rangle^2} / \langle T \rangle \tag{3}$$

where $\Delta x^2 = (x - \langle x \rangle)^2$ denotes here and in the following the square displacement of a stochastic quantity. The CV is small for a regular periodic sequence of spikes and large for irregular spiking (a Poisson spike train yields $R = 1$).
Second, we may look at the power spectrum of $v(t)$

$$N(\omega) = \lim_{T \to \infty} \langle | \int_0^\infty dt v(t) e^{i\omega t} |^2 \rangle / T \tag{4}$$

that reveals a peak versus frequency ω in case of present oscillations.
We can also study the statistics of the pulse number (spike count) $n(T)$ in a time window $(0, T)$. Of special interest for regularity of spiking is the growth of variance in time characterized by the diffusion coefficient of the pulse number

$$D_{\text{eff}} = \lim_{T \to \infty} \langle \Delta n^2(T) \rangle / (2T). \tag{5}$$

A slight growth of variance, i.e. a small value of D_{eff}, indicates clearly a regularity of the single spike count process $n(T)$ and thus serves as another measure to characterize coherence resonance.
The two-state approximation which permits us to calculate all those quantities analytically has been worked out in two recent papers [2, 3] (see also [4] for more details); here we just sketch this derivation. In case of a perfect time scale separation, i.e. for $\tau \to 0$ in eq. (1), the system stays on the two stable branches (the left and right ones) of $F(v)$, it may, however, switch between these branches (this is illustrated in Fig. 1, l.h.s.) In this limit we can set $\dot{v} = 0$ in eq. (1) which yields a two valued function $v = F_{L,R}^{-1}(u)$ and hence two different Langevin equations (second one of eqs. 1) corresponding to the motion on the left and right branch, respectively. Trajectories on the left (right) branch that reach the minimum $u_- = F(v_-)$ (maximum $u_+ = F(u_+)$) of $F(v)$ are absorbed and infinitely fast reinjected at the corresponding point on the right (left) branch (see Fig. 1, middle panel) The potentials that govern the dynamics on each branch can be read off from the respective Langevin equations:

$$U_{L,R}(u) = (u - b)^2/2 - \gamma \int^u du' F_{L,R}^{-1}(u'). \tag{6}$$

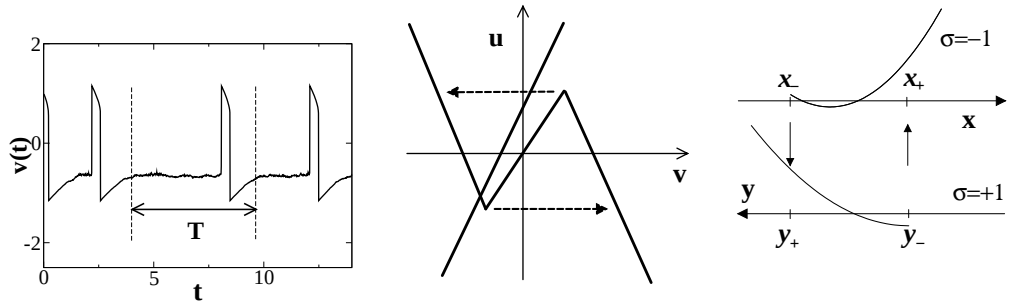

FIGURE 1. Left:sample trajectory of voltage variable with interspike interval indicated by the arrow. Middle: Piecewise linear null clines (eq. (2)) and possible transitions (arrows) for small τ. Right: two-state model with transition points, effective potentials (thin lines) and values attained by $\sigma(t)$.

Although their specific shapes depend on the function $F(v)$, there is an important difference between $U_L(u)$ and $U_R(u)$ (cf. Fig. 1,r.h.s.): while on the left branch we obtain a minimum in the potential that corresponds to the fixed point in the two-dimensional dynamics, for the potential on the right branch only a monotonous potential results. Under these conditions the system can escape from the left branch only by the assistance of noise while the right branch is left in a finite time ("downhill" motion until the absorbing boundary is reached) even in the absence of noise.
We may associate a discrete variable $\sigma(t) = \mathrm{sgn}[v(t)]$ with the branch currently occupied, i.e. we approximate the excitable dynamics by a two-state model for which the waiting time in each state is governed by a Langevin dynamics and an absorbing boundary. The interspike interval consists of the sum of the subsequent passage times along the left and right branches. These times are statistically independent, therefore the spike train (the instants at which $\sigma(t) = -1 \to +1$) forms a *renewal process* [5]. For such a process, CV and diffusion coefficient of the pulse number can be expressed by the moments of the aforementioned passage times as follows

$$R = \sqrt{\langle \Delta T_L^2 \rangle + \langle \Delta T_R^2 \rangle} / (\langle T_L \rangle + \langle T_R \rangle) \ , \ 2D_{\mathrm{eff}} = (\langle \Delta T_L^2 \rangle + \langle \Delta T_R^2 \rangle) / (\langle T_L \rangle + \langle T_R \rangle)^3. \quad (7)$$

The moments of the passage times can be calculated using the classical quadrature formulae for the problem (see, e.g., [6, 4])

$$\langle T_{L,R} \rangle = \int_{u_-}^{u_+} dx \, I_{L,R}(x) \ , \quad I_{L,R}(x) = \frac{1}{D} e^{V_{L,R}(x)/D} \int_{-\infty}^{x} dy \, e^{-V_{L,R}(y)/D}, \quad (8)$$

$$\langle \Delta T_{L,R}^2 \rangle = 2 \int_{-\infty}^{u_+} dz \, [I_{L,R}(z)]^2 e^{-V_{L,R}(z)/D} \int_{z}^{u_+} dx \, \Theta(x - u_-) e^{V_{L,R}(x)/D} \quad (9)$$

with $V_R(x) = U_R(x)$, $V_L(x) = U_L(-x)$ and u_- and u_+ are the local minimum and maximum of the function $F(v)$, respectively. The quadrature results for CV and diffusion coefficient in the system with cubic null cline are shown in Fig. 2 and also compared

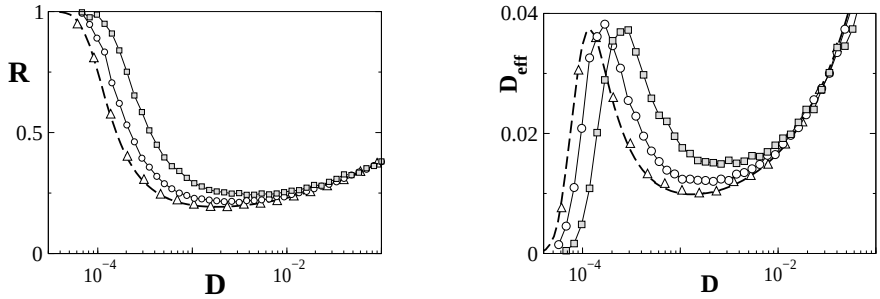

FIGURE 2. Coeffi cient of variation (left) and diffusion coeffi cient of spike count (right) versus noise intensity D for the FN model with cubic nonlinearity at $\gamma = 1.5, b = 0.6$. Approximation (dashed line) compared to simulations with $\tau = 10^{-3}$ (squares), $\tau = 10^{-4}$ (circles) and $\tau = 0$ (triangles).

to simulation results of the full dynamics at different values of the time scale separation constant τ. Both functions attain minimal values at a fi nite intensity of the applied noise indicating coherence resonance. Although there are only slight differences between approximation and numerical results, we would like to point out that CV and D_{eff} for small time scale separation reveal slightly deeper minima than the simulation results for fi nite τ. This means that a better time scale separation implies a more pronounced coherence. We note that while changing the systems parameters a minimum in CV is easy to obtain, the minimum in D_{eff} occurs only in case of strong excitability, i.e. just in the case where the CR effect is strongly pronounced. The diffusion coeffi cient of pulse number therefore constitutes a strong criterion of coherence resonance (see also [4], chapter 1.1).
The power spectrum of $\sigma(t)$ can be obtained applying Stratonovich's formula for a general two-state process [7] (we omit the δ peak at $\omega = 0$ due to a fi nite mean of $\sigma(t)$)

$$N(\omega) = \frac{8J_0}{\omega^2}\Re\left(\frac{(1-w_L(\omega))(1-w_R(\omega))}{1-w_L(\omega)w_R(\omega)}\right). \tag{10}$$

where $J_0 = 1/(\langle T_L + T_R\rangle)$ and $w_{L,R}(\omega)$ are the characteristic functions for the times T_L and T_R, respectively. For the piecewise linear nullclines eq. (2) these functions can be calculated

$$w_L(\omega) = e^{\frac{x_+^2 - x_-^2}{4\tilde{D}}}\frac{\mathscr{D}_{-i\omega}(x_+/\sqrt{\tilde{D}})}{\mathscr{D}_{-i\omega}(x_-/\sqrt{\tilde{D}})}\,,\;\; w_R(\omega) = e^{\frac{y_+^2 - y_-^2}{4\tilde{D}}}\frac{\mathscr{D}_{-i\omega}(y_+/\sqrt{\tilde{D}})}{\mathscr{D}_{-i\omega}(y_-/\sqrt{\tilde{D}})}. \tag{11}$$

Here $\mathscr{D}_a(z)$ is the parabolic cylinder function [8] and we use rescaled time $\tilde{t} = (\gamma+1)t$ and noise intensity $\tilde{D} = D/(1+\gamma)$ [3]. The $x_\pm, y_\pm$ are given by

$$x_\pm = \pm 1/2 - (b-\gamma)/(1+\gamma)\,,\; y_\pm = \pm 1/2 + (b+\gamma)/(1+\gamma) \tag{12}$$

The power spectrum resulting from these equations is shown for $\gamma = 1$, $b = 0.4$ and different noise levels in Fig. 3 (l.h.s.). While for small and large values of the noise intensity the spectrum falls off monotonously, at intermediate noise strength a peak versus frequency is obtained. This noise-induced eigenfrequency is another manifestation of

coherence resonance. A comparison between this frequency and that given by the inverse mean interspike interval $\omega_m = 2\pi/\langle T\rangle$ is made in a counter plot in Fig. 3 (l.h.s., inset). Clearly, the noise-induced eigenfrequency is slightly larger than the mean frequency. In case of coherence resonance, however, both frequencies approach each other.

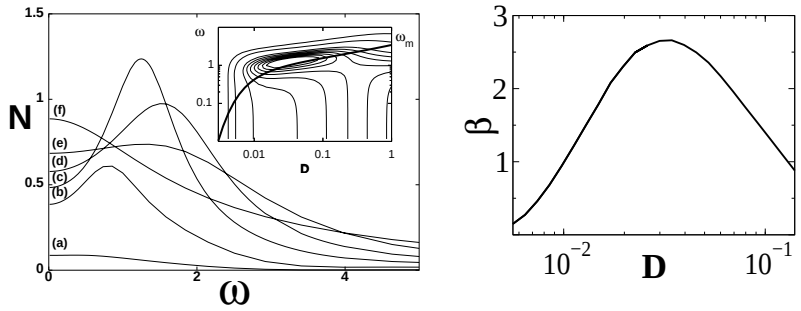

FIGURE 3. Left: output spectrum of the excitable system versus frequency and different noise levels (a)-(f): $\tilde{D} = 0.004, 0.009, 0.033, 0.094, 0.207, 0.769$. Inset: Contour plot of spectral density versus D and ω compared to mean frequency $\omega_m(\tilde{D})$ (thick line). Right: degree of coherence vs noise intensity.

We can measure the coherence of the oscillation by the so called degree of coherence

$$\beta = \frac{N(\omega_{max})}{(\omega_1 - \omega_2)/\omega_{max}} \quad \text{with} \quad N(\omega_1) = N(\omega_2) = N(\omega_{max})/a\,,\ \omega_1 < \omega_{max} < \omega_2 \quad (13)$$

Here, we choose $a = 1.2$, however, the value of a has no impact on the principal dependence of β on D. As can be seen this function (numerically calculated from eq. (10) and eq. (11)) attains a maximum versus noise intensity. A comparison to CV and D_{eff} curves for the system with piecewise linear null cline (not shown) reveals that all measures of CR attain their extremal value at roughly the same noise intensity if coherence resonance is strongly pronounced. For a weak CR effect, the minima of CV and D_{eff} and the maximum in the degree of coherence are attained at slightly different values that will depend on the specific definitions of the respective measure, e.g. the factor a in the above definition of β.
We note that the two-state description can be also used to calculate the linear response of the stochastic FN model with respect to periodic stimulation. In this case a possible functional role of coherence resonance becomes apparent - resonances with the noise-induced eigenfrequency might be useful for signal transmission through a neuron (see also [9, 10]).

CLUSTER OF STOCHASTIC CALCIUM CHANNEL

Next we consider as an application for an oscillating excitable dynamics a single cluster of calcium releasing ion-channels. Calcium plays the role of an important intra- and intercellular messenger in all types of cells and tissues. The elevation of free intracellular calcium concentration is due to the opening of calcium stores, e.g. the endoplasmatic reticulum (ER), which are gated by ion channels. Of importance for many intracellular processes is the family of inositol-(1,4,5)-triphosphate receptor (IP_3R) channels, for a

review see [11], which is present in several types of tissues, e.g. neuronal tissue and smooth muscles.
We follow the idea that a certain number of ion channels in the cluster creates a necessary common level of noise which determines the stochastic dynamics of the whole cluster [12, 13, 14]. A mean fi eld description of the calcium concentration, which is governed by fluctuations in the open probability of subunits, will show that the level of fluctuations, i.e. the number of channels in the cluster, plays the crucial role for the stochastic dynamics [15]. The power spectrum reveals collective stochastic calcium oscillations in the cluster which become most regular for an optimally selected noise level.
One channel is composed of four homolog subunits, each of which is activated by IP_3 and shows a bell shaped activation dependence on the calcium concentration [16], thus calcium induces and limits its own release. De Young and Keizer incorporated this to an eight-state model [17] which was later reduced to a two-state system (Li-Rinzel model) for this receptor [18, 19]. We apply the Li-Rinzel model for a single cluster of N_0 subunits, i.e. $N_0/4$ channels. The channel interaction is assumed to be instantaneous via the spatially homogeneous calcium concentration c=[Ca^{2+}] which is assumed to be realized by fast intracellular calcium diffusion. One channel is open if at least three out of four subunits are in the activated state [20],

$$P_{\text{open}} = x^4 + 4x^3(1-x)\,, \qquad x = \frac{pc(1-y)}{(p+K_1)(c+K_5)}\,, \tag{14}$$

where y is the probability of the subunit being calcium inactivated and p=[IP_3] is the concentration of the ligand IP_3.
If N of the N_0 subunits are in the inactivated state, a Master equation for the dynamics of inactivation can be formulated

$$\begin{aligned}\frac{\partial P(N,t)}{\partial t} &= -\left((N_0-N)K^+ + NK^-\right)P(N,t) \\ &+(N_0-N-1)K^+P(N-1,t) + (N+1)K^-P(N+1,t)\,.\end{aligned} \tag{15}$$

Therein the rate of inactivation $K^+(c)$ depends on the calcium concentration whereas the activation process, K^-, does not

$$K^+(c) = \frac{2c(K_1k_1k_4 + k_2k_4c + k_1k_2p)}{c(k_2+k_4) + 2k_1(K_1+p)}\,, \quad K^- = \frac{2(k_{-3}k_{-4} + k_{-2}(k_{-4}+k_3p))}{k_{-2}+k_{-4}+2k_3(K_3+p)}\,. \tag{16}$$

Eq. (15) can be expanded for $N \gg 1$ to give a Fokker-Planck Equation. The latter in turn is equivalent to the Langevin Equation

$$\dot{y} = (1-y)K^+ - yK^- + \sqrt{\frac{(1-y)K^+ + yK^-}{N_0}}\,\xi(t) \tag{17}$$

where $\xi(t)$ is zero-mean, Gaussian white noise, $\langle \xi(t)\xi(t+\tau)\rangle = \delta(\tau)$ and scales with an intensity inversely proportional to the number of clustering channels.

The intracellular calcium concentration is determined by

$$\dot{c} = (r_1 P_{\text{open}} + r_2)(c_{\text{ER}} - c) - r_3 \frac{c^2}{c^2 + K_p^2}, \qquad c_{\text{ER}} = (C_0 - c)/\alpha. \tag{18}$$

The first term models the gradient-dependent influx (Ca^{2+} source) while the second term represents the activity of the SERCA-pump (Ca^{2+} sink) which re-establishes this gradient; r_1, r_2 and r_3 are channel, leak and pump fluxes, respectively, c_{ER} is the ER calcium concentration, α is the ratio of ER volume to cell volume and C_0 is a constant, representing a local condition for a fixed amount of total cell calcium; our numeric standard parameters, including the dissociation constants $K_i = k_{-i}/k_i$, are given in [22]. Most of them are taken from [17, 21], some were adopted to new measurements [23] and some were slightly change by us to investigate other regimes.

To find an analytic description we have carried out further simplifications [15]: i) perfect time scale separation, ii) linear nullcline approximation, and iii) replacement of phase state dependent noise by additive noise with level taken in the fixed point $(c^s, y^s) = (0.076\,\mu M, 0.0802)$. This defines a two-state process switching between low and high intracellular calcium concentration. Shuai et al. [14] numerically described this process and computed its spectrum. We used the results of the piecewise linear FN model to find an analytic description [15].

The spectrum for the linearized system shows the same properties as Fig. 3, additionally the second harmonics of the peak are present. There exists an intermediate noise level for which the degree of coherence eq. (13) reaches a maximum value, for the corresponding number of channels calcium signalling can be considered most regular.

To prove the validity of our simplification we performed stochastic simulations of the unreduced Li-Rinzel model. Each of the four channel subunits was treated according to the Li-Rinzel model, i.e. the process $y(t) = 0$ or 1, to decide for a transition between these two states a uniformly distributed random number $\rho \in [0,1]$ was drawn and if $\rho \mathrm{d}t < K^{\pm}$ the subunit made the corresponding transition. For non-inhibited subunits the probability of being in the open-state is given by eq. (14) and the open state was set if $\rho' < x$, where ρ' is another. A channel opens if three or four subunits are in the open-state and the fraction N^{open}/N_0 of open channels substituted P_{open} in eq. (18). The evolution of $c(t)$ was sampled with $\mathrm{d}t = 0.01\,s$ for a time $T = 2621.44\,s$ and the time series was then zero averaged and fast Fourier transformed (with 2^{18} points). In order to obtain a smooth power spectrum we averaged over 300 runs. Results are displayed in Fig. 4(left). For a single channel (maximal noise level) the spectrum shows no peak but monotonously falls off for increasing frequencies. If the number of channels is increased, i.e. the system noise reduced, a peak emerges, reaches a maximum value and later starts to disappear again for very large clusters. Thus, the simulations show the same qualitative behavior as the reduced model shown on the r.h.s. in Fig. (4). To answer the key question – what is the optimal channel number per cluster with respect to signalling periodicity – we calculated the degree of coherence of the stochastic oscillations from eq. (13) with $a = 2$. The comparison of analytic and stochastic calculation is given in Fig. 4 (left) and shows excellent agreement.

In a numeric first approach similar results were obtained in [12, 13, 14] which showed the existence of a certain range of cluster size where signaling properties become most

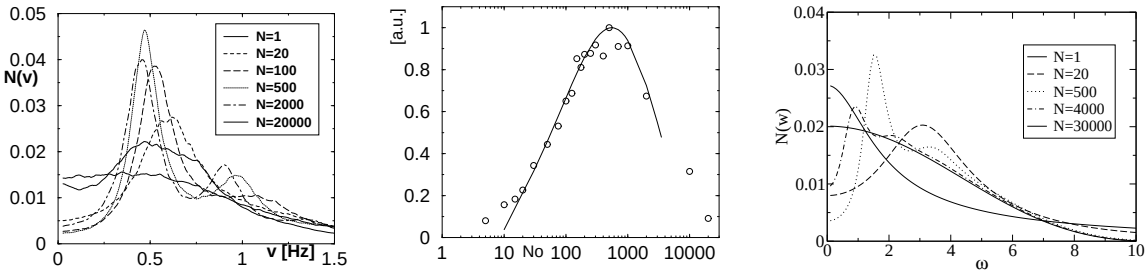

FIGURE 4. Left: Power spectra (left: simulations, right: analytic), degree of coherence [middle; stochastic simulation (circles) compared with analytic model (line)].

periodic and in this work we presented analytic evidence for that in a cluster of IP_3R-I calcium ion channels. We found a range of 20-750 channels per cluster optimal for signaling periodicity. The key parameter is the cluster size, i.e. the number of channels, governing the fluctuations in the clusters mean open probability.

This work was supported by DFG-Sfb 555 and Gk 268.

REFERENCES

1. A. Pikovsky and J. Kurths, *Phys. Rev. Lett.* **78**, 775 (1997).
2. B. Lindner and L. Schimansky-Geier, *Phys. Rev. E* **60**, 7270 (1999).
3. B. Lindner and L. Schimansky-Geier, *Phys. Rev. E* **61**, 6103 (2000).
4. B. Lindner, *Coherence and Stochastic Resonance in Nonlinear Dynamical Systems* (Logos-Verlag, Berlin, 2002).
5. D. R. Cox, *Renewal Theory* (Methuen, London, 1962).
6. C. W. Gardiner, *Handbook of Stochastic Methods* (Springer-Verlag, Berlin, 1985).
7. R. L. Stratonovich, *Topics in the theory of random noise*, vol.1, p.175 (Gordon and Breach, New York, 1963).
8. M. Abramowitz and I. A. Stegun, *Handbook of Mathematical Functions* (Dover, New York, 1970).
9. B. Lindner and L. Schimansky-Geier, *Phys. Rev. Lett.* **86**, 2934 (2001).
10. B. Lindner, L. Schimansky-Geier, and A. Longtin, *Phys. Rev. E* **66**, 031916 (2002).
11. Y. Yoshida, and S. Imai, *Jpn. J. Pharmacol.* **74**, 125 (1997).
12. P. Jung, and J. W. Shuai, *Europhys. Lett.* **56**, 29 (2001).
13. G. Schmidt, I. Goychuk, and P. Hänggi, *Europhys. Lett.* **56**, 22 (2001).
14. J.W. Shuai and P. Jung, *Phys. Rev. Lett.* **88**, 068102 (2002).
15. L. Meinhold and L. Schimansky-Geier, *Phys. Rev. E*, in print.
16. I. Bezprozvanny, J. Watras, and B.E. Ehrlich, *Nature* **351**, 751 (1991).
17. G.W. De Young and J. Keizer, *PNAS* **89**, 9895 (1992).
18. G.W. De Young and J. Keizer, *J. theor. Biol.* **166**, 431 (1994).
19. Y.X. Li and J. Rinzel, *J. theor. Biol.* **166**, 461 (1994).
20. J. Watras, I. Bezprozvanny, and B.E. Ehrlich, *J. Neurosci.* **11**, 3239 (1991).
21. M. Falcke, L. Tsimring, and H. Levine, *Phys. Rev. E* **62**, 2636 (2000).
22. Numeric model parameter: $K_1 = 0.0785\mu M$; $K_2 = 1.049\mu M$;$K_3 = 0.312\mu M$; $K_4 = 0.26393\mu M$; $K_5 = 0.0823\mu M$; k_1=400.0$(\mu M s)^{-1}$; k_2=0.3$(\mu M s)^{-1}$; k_3=400$(\mu M s)^{-1}$; k_4=0.3$(\mu M s)^{-1}$; k_5=80$(\mu M s)^{-1}$; $r_1 = 0.4 s^{-1}$; $r_2 = 0.02 s^{-1}$; $r_3 = 2.1(\mu M s)^{-1}$; $K_p = 0.08\mu M$; $C_0 = 2.0\mu M$; $p = 1.15\mu M$; $\alpha = 0.185$.
23. H. Yoneshima, A. Miyawaki, T. Michikawa, T. Furuichi, and K. Mikoshiba, *Biochem. J.* **322**, 591 (1997).